Possibility of creating a laser source operating in 0.2 to 12.0 μm wavelength region

Yu.M. Andreev and P.P. Geiko

Institute of Optical Monitoring,
Siberian Branch of the Russian Academy of Sciences, Tomsk

Received November 9, 2001

The possibility is considered of creating, based on nonlinear crystal optics, an all-solid-state source of coherent radiation in the region of 0.2 to 12.0 μm intended for use in a general-purpose gas-aerosol lidar. It is shown that the use of parametric frequency converters of Nd:YAG, holmium, and erbium laser radiation enables one to develop such a source with the parameters meeting its practical implementation. For the mid-IR region we propose to use nonlinear $HgGa_2S_4$ crystals, doped GaSe:In crystals, and new $AgGa_xGe_{1-x}S_4$ and $Hg_{(1-x)}Cd_xGa_2S_4$ mixed crystals that have been poorly studied yet. Some results of a thorough research of the linear and nonlinear optical properties of these crystals are presented. In the rest part of the region considered, it is proposed to use commercial frequency converters based on LBO, KTA, KTP, and BBO crystals.

1. State of the art of the research

Two main problems of real-time remote monitoring of the ecological state of the atmosphere that can be solved with lidar systems involve determination of relative content of aerosol and gas components of natural and anthropogenic origin. It is worth monitoring fine fraction of natural aerosol in the shortwave part of the atmospheric transmission spectrum down to 200 nm wavelength, while the coarse fraction can be monitored in the near-IR and mid-IR spectral regions at the wavelengths up to 10 μm and longer, since the interfering effect of the fine aerosol of natural origin is minimum in this case. For monitoring of the gas composition of the atmosphere, the differential absorption lidar (DIAL) method has received wide recognition.

Remote sensing of nitrogen oxides, O_3, and SO_2 is traditionally conducted with dye and excimer lasers operating in the region of 0.28 to 0.35 μm. In the visible spectral region, monitoring of only NO_2 is possible, for example, with argon-ion lasers. In the near-IR region, methane can be monitored within its 1.33, 1.57, 1.65, and 2.32 μm absorption bands and semiconductor lasers or optical parametric oscillators (OPO). In the mid-IR, the total content of methane and light hydrocarbons can be determined with the use of complex-design multistage OPOs based on $LiNbO_3$, KTP, and KTA crystals and the intense absorption band centered at 3.3 μm. At 30–100-m paths, low-power two-frequency He–Ne lasers can be successfully used for monitoring of the methane content. Componentwise analysis of the content of ethylene and a large number of light hydrocarbons, as well as ozone is conducted with high-power CO_2 lasers operating in the region of 9 to 11 μm. In other words, almost all known laser systems operating in the region of 0.2–12.0 μm were tested as lidar components, but their common disadvantage has not yet been overcome.

No versatile lidar has been created so far capable of solving the above-mentioned problems to a practically acceptable degree. The practically sufficient degree means here the possibility of simultaneously monitoring fine and coarse aerosol fractions and most abundant gaseous pollutants: nitrogen oxides, sulfur and carbon oxides, ozone, methane, and other light hydrocarbons. The longwave boundary of the considered region (12 μm) was selected primarily because lidars operating at longer waves require application of radiation detectors that must be cooled with liquid helium, for which reason they did not receive wide acceptance.

Earlier it was shown that use of efficient single- and two-stage parametric frequency converters (PFC) based on $ZnGeP_2$ crystals allows the mid-IR region to be spanned with the frequency-converted CO_2-laser lines with the step of 10^{-3} cm^{-1}, and the restriction on the number of monitored gases is thus lifted.[1] Table 1 presents the parameters of some commercial narrow-band PFCs continuously tunable in a wide spectral range that provide for extra capabilities in realization of lidar gas analysis and were available in the USA in 2000 (Ref. 2). It can be seen that the UV, visible, and near-IR regions can be fully covered with the use of nonlinear crystal optics, in particular, with a widely used and well-developed lasers as a pump source. These results follow from previous successful investigations. Thus, the second harmonic generation (SHG) of a Nd:YAG laser emission has been achieved in a 14-mm long LBO crystal with the efficiency of 70% in the pulsed mode and 36% at continuous wave pumping and the second harmonic power of higher than 6 W. An optical parametric oscillator pumped with the third harmonic of a Nd:YAG laser radiation covered the region of 0.416–0.487 and 1.306–2.411 μm at the total efficiency of 35%, and so on.[3]

0235-6880/02/07 557-07 $02.00

Table 1. Parameters of commercial optical parametric oscillators operating in the UV, visible, near-IR, and mid-IR spectral regions

Model	Manufacturer	Tuning range, μm	Power/energy	Pulse repetition rate, Hz	Pulse duration, ns	Pumping	Band width	Notes
MOPO-HF	Spectra Physics	0.44–1.8	75 mJ	10	4–6	Nd:YAG	0.075 cm^{-1}	OPO autotracking
BBO-3BII	U-Oplaz Tech. Inc.	0.2–4.0	100 mJ	1–100	1–10	Nd:YAG	–	Single-frequency OPO
1100	Aculight Corp.	1.39–4.7	3–30 μJ	$2 \cdot 10^4$	10	Diode	10 MHz	OPO
DFG	Coherent Inc.	3.0–10.0	3 mW	$3 \cdot 10^5$	$< 1.5 \cdot 10^{-4}$	Model Rega 9000	–	OPO

According to Table 1, the first commercially available OPO operating in the mid-IR has appeared. However, this situation still does not solve the problem formulated. A radiation source needed for versatile gas-aerosol lidars should operate in the repetitively pulsed mode, be tunable in the region from 0.2 to 12.0 μm, and have a narrow, as compared with the gas absorption lines, band ≤ 0.1–0.01 cm^{-1}, pulse duration of 5–20 ns, and the pulse repetition rate no less than 1 kHz. These parameters provide high sensitivity and spatial resolution and allow measurements under the so-called conditions of "frozen" atmosphere. To obtain the sensing range of 1 to 10 km, the energy per single pulse should be 1 to 50 mJ and higher at high performance characteristics, low power consumption, small size, and low price.

However, low efficiency, low optical damage threshold, and high optical losses in widespread nonlinear crystals at the wavelengths of solid-state pump lasers do not allow such radiation sources to be created with the use of nonlinear crystal optics. The shortwave part of the mid-IR region (2.5–12.0 μm) presents a real challenge.[4] The most significant fact is that all the known nonlinear crystals of the mid-IR region: Te, $CdGeAs_2$, $ZnGeP_2$, Tl_3AsSe_3, $AgGaSe_2$, $AgGa_{(1-x)}In_xSe_2$, and CdSe, have high optical losses or are opaque in the spectral range of 1–3 μm. Application of mid-IR OPOs based on $ZnGeP_2$ crystals with the optical properties improved by after-growth processing and broadband GaSe crystals seems to be rather promising. The mean output pulse power of original, but non-commercial first versions of OPOs achieved 16.5 W (Ref. 5). Low nonlinear properties of GaSe crystals (as well as $AgGaS_2$ crystals) transparent in the major portion of the visible region cause low efficiency and output power parameters of the second OPO, despite that their spectrum covers all atmospheric transmission windows in the range of 2.3 to 18 μm (Ref. 6). It should be noted that it is too unlikely to find new lasing media.

The aim of this work was to study the possibility of creating an all-solid-state small-size radiation source capable of emitting in the region of 0.2 to 12.0 μm based on the solid-state Nd:YAG, holmium, or erbium lasers by methods of nonlinear crystal optics with the use of poorly studied and new nonlinear crystals.

2. The approach proposed

Figure 1 shows the layout of the proposed source with two groups of nonlinear crystals used. The LBO, KTA, KTP, and BBO crystals form the first group of crystals used for solid-state laser frequency conversion into the UV, visible, and near-IR spectral regions through harmonic generation and OPO initiation by pumping with a harmonic or difference frequency radiation. The capabilities of frequency converters based on these crystals are not considered here because the situation with their development is fairly well known. The second group incorporates poorly studied $HgGa_2S_4$ crystals,[7] doped GaSe:In crystals,[8] as well as new $AgGa_xGe_{1-x}S_4$ and $Hg_{(1-x)}Cd_xGa_2S_4$ mixed crystals.[9] These all are potential candidates for the solid-state laser frequency conversion into the mid-IR region according to data on their transmission spectrum available. To evaluate the capabilities of the corresponding frequency converters, consider first the physical properties of this group of crystals.

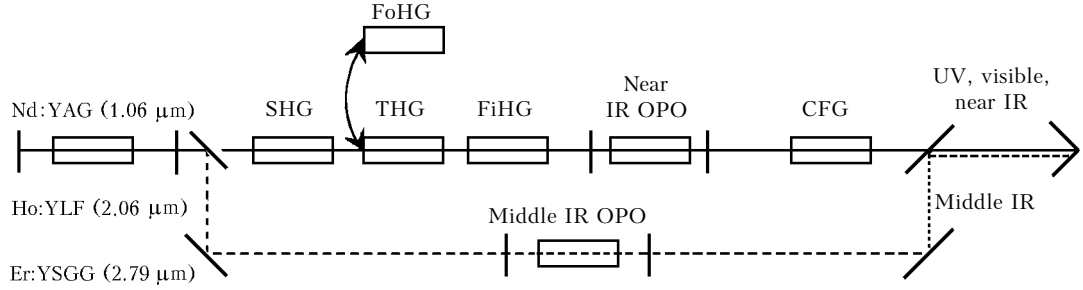

Fig. 1. Radiation source covering the range of 0.2–12.0 μm. SHG, THG, FoHG, FiHG are second, third, fourth, and fifth harmonic generators, CFG is combined (sum and difference) frequency generator.

3. Optical properties of new nonlinear crystals

The progress achieved in the crystal growth technology allowed us to study physical properties of new nonlinear crystals. Optical properties in the UV, visible, and near-IR regions were studied with a Shimadzu UV-3101PC spectrophotometer having a ∅2 mm diaphragm and a polarization attachment. For the measurements in the mid-IR region, we used a Specord 80 M spectrophotometer. The microelectronic-emission analysis was carried out with a Jeol electronic microscope (Japan) and a Link spectroscopic attachment (Germany).

The transmission spectrum of a 10 × 12 × 3.1 mm two-phase (yellow and orange phases) sample of the $HgGa_2S_4$ crystal of relatively high optical quality is shown in Fig. 2*a*. The shortwave boundary of its transmission spectrum at the zero level lies nearby 490 nm for the yellow phase and 507.5 nm for the orange phase. The longwave boundaries of the transmission spectra of both phases do not differ and lie in the region of 15.5–16.0 μm (Fig. 2*b*).

For 10% level, they are, respectively, 510 and 525 nm in the shortwave part of the spectrum and 13.3–13.4 μm in the longwave part. Variations of the transmittance level in different parts of the crystal did not exceed 5% at acceptable variations of the composition $Hg_{(1\pm0.10)}Ga_{(2\pm0.085)}S_{(4\pm0.067)}$. The upper boundary of the optical loss coefficient in the region of maximum transmittance was estimated as $\alpha \le 0.1–0.2$ cm^{-1}, that is quite acceptable for creation of high-efficiency frequency converters. It should be noted that the loss at the wavelengths of the 9-μm CO_2 laser band due to phonon absorption is comparable with and even smaller than the corresponding loss in $ZnGeP_2$. Besides, it is no higher than the level of losses in the best $LiInS_2$ crystals.[10] From the refractive index measured by the method of least deflection angle, we have found the dispersion dependences, which were approximated by the Sellmeier dispersion formulas. The coefficients of these formulas are given in Table 2.

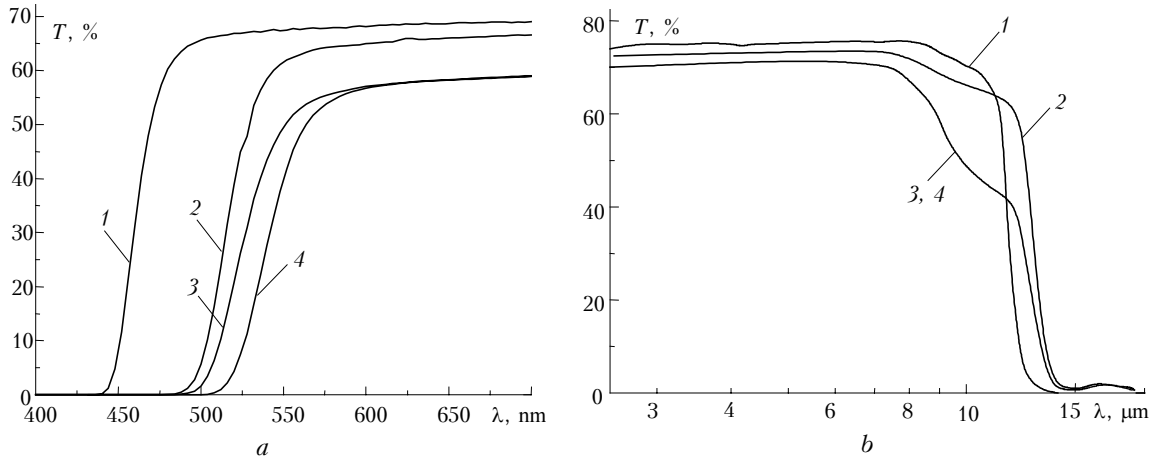

Fig. 2. Transmission spectra of 2.1-mm $AgGaGeS_4$ crystal (*1*), 2.1-mm $Cd_{0.35}Hg_{0.65}Ga_2S_4$ crystal (*2*), and 3.1-mm $HgGa_2S_4$ crystal: yellow (*3*) and orange phases (*4*), in the visible (*a*) and longwave parts of the spectrum (*b*).

Table 2. Sellmeier coefficients for new nonlinear crystals

Crystal	n	Parameter				
		A_1	A_2	A_3	A_4	A_5
$HgGa_2S_4$	n_o	3.44830	2.47671	0.09569	0.28314	250
(orange phase)	n_e	3.39566	2.33212	0.09215	0.28125	250
$HgGa_2S_4$	n_o	3.24284	2.69562	0.09166	396530	1500
(yellow phase)	n_e	3.07682	2.69992	0.08527	3.80133	1500
GaSe:In*	n_o	7.45247	0.37683	0.09305	0.00164	–
	n_e	5.77794	0.20685	0.24772	0.00128	–
$Hg_{(1-x)}Cd_xGa_2S_4$	n_o	2.72321	2.87028	0.07336	3.23820	1300
(x = 0.4)	n_e	2.79539	2.69431	0.07400	3.29752	1300
$AgGaGeS_4$ or	n_z	5.34460	0.17565	−0.07214	−0.00255	–
$Ag_xGa_xGe_{(1-x)}S_4$*	n_x	5.31103	0.18103	−0.06927	−0.00231	–
(x = 0.5)	n_y	5.07772	0.16277	−0.06148	−0.00157	–

* In these cases the Sellmeier formulas have the form: $n^2 = A_1 + A_2/(\lambda^2 - A_3) - A_4\lambda^2$, in other cases $n^2 = A_1 + A_2\lambda^2/(\lambda^2 - A_3) + A_4\lambda^2/(\lambda^2 - A_5)$, λ is the wavelength, in μm.

We do not know any publications describing the dispersion dependences of the crystals studied in this paper. The only exclusion is $HgGa_2S_4$, whose Sellmeier coefficients are given in recent edition of the Handbook of Nonlinear Optical Crystals[3] though without specifying the phase. It should be noted that calculations of the phase-matching angles with the use of these data and our data for the orange phase of $HgGa_2S_4$ give close results (the difference in the phase-matching angles is no larger than 1°), in spite of a quite large difference in the coefficients.

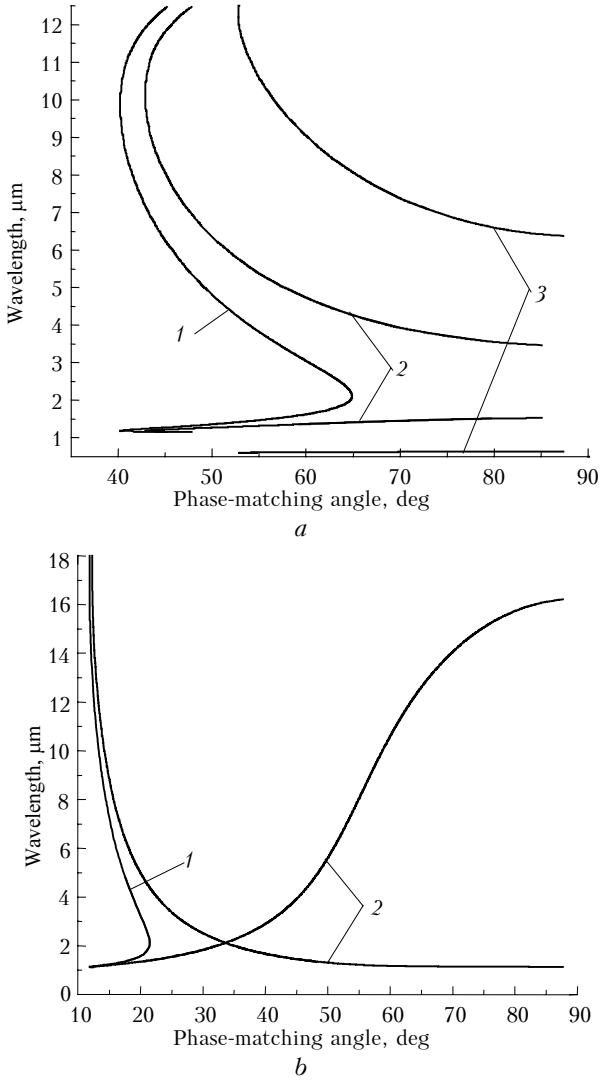

Fig. 3. Phase-matching diagrams for an OPO pumped at $\lambda = 1.06$ μm by the first (*1*) and second (*2*) types of interaction and $\lambda = 0.578$ μm, first type (*3*) in $HgGa_2S_4$ (*a*). The same at $\lambda = 1.06$ μm for the first (*1*) and second (*2*) types in GaSe:In (*b*).

Analysis of the phase-matching conditions calculated with the use of the dispersion dependences obtained showed the possibility of initiating the mid-IR OPO based on $HgGa_2S_4$ pumped by solid-state lasers, in particular, Ti:Al_2O_3 and even copper-vapor lasers, as well as the second harmonic generator of the 9-μm CO_2-laser band. Figure 3*a* shows the calculated tuning curves for an OPO pumped by radiation at the wavelength $\lambda = 1.06$ μm for two possible types of interaction (*e–oo* and *e–eo*) and by a copper-vapor laser ($\lambda = 0.578$ μm, *e–oo* interaction) in the orange phase of $HgGa_2S_4$.

The calculated and experimental phase-matching angles for the SHG 9*P*(20) line of TEA CO_2 laser at the wavelength of 9.55 μm for the I (*oo–e*) interaction in this crystal phase agree well (67°07′ and 67°20′), thus confirming the correctness of determination of optical properties and the estimates obtained, but they are somewhat lower than the values expected for the yellow phase (67°50′ against 70°39′).

The coefficients of the quadratic nonlinear susceptibility of $HgGa_2S_4$ were estimated as $d_{36} = 35$ and $d_{31} = (15 \pm 15)\%$ pm/V for both of the crystal phases. The estimate was obtained by the well-known method of comparison[5] of, in this case, the efficiency of CO_2 laser SHG in plates of the crystals studied and in the $ZnGeP_2$ crystal. The value of d_{36} for $ZnGeP_2$ was taken equal to 75 pm/V (Ref. 3). The nonlinear coefficients were re-calculated with the allowance made for difference in the phase-matching angles and different equations for the effective nonlinear coefficients in the $HgGa_2S_4$ and $ZnGeP_2$ crystals. These equations are given below.

The GaSe crystals of the point symmetry group 6*m*2 have an extremely wide transmission region from 0.65 to 19.0 μm and high birefringence $B = 0.375$. The level of optical losses in the maximum transmittance window is $\alpha \le 0.05–0.1$ cm^{-1}. High heat conductivity of these crystals in the layer plane [0.162 W/(cm · deg)], simple growth technology, and, consequently, relatively low price favor creation of high-efficiency OPOs based on them. Nevertheless, these crystals did not receive wide use. The pronounced anisotropy of mechanic and thermal properties caused by their layered structure hinders in processing of working surfaces and production of optical elements with arbitrary orientation. Elements can be produced only by ordinary easy detachment of a part of an ingot grown. By the same cause, working elements are easily deformable by light mechanical effects and vibrations.

But the most significant cause is low nonlinear susceptibility $d_{22} = 23$ pm/V. It is just for this reason why low efficiency was observed experimentally for optical parametric oscillators, CO_2 laser second harmonic, and parametric luminescence.[11] On the other hand, high, up to 75 pm/V, nonlinear susceptibility was reported in some earlier papers.[8] Determination of the true value of this parameter is of principle importance for finding the place of GaSe crystals in nonlinear optics.

References 8 and 12 made the situation much clearer. It was found that in a thin (100 μm) samples of GaSe the nonlinear susceptibility d_{22} is 70 pm/V, and its value decreases as the sample thickness increases. This points to masking of natural nonlinear properties by poor cleavage of layers. Doping with indium (0.3–1.0%) drastically improved mechanical properties of

this crystal. Microhardness increased by an order of magnitude, and this made it possible processing, in particular, polishing of GaSe crystals by ordinary methods and fabrication of elements with any orientation.

The eightfold difference in the heat conductivity of GaSe crystals in the layer plane and in the plane normal to it decreased almost four times. Figure 3*b* depicts the tuning curves for parametric generation in GaSe:In pumped at $\lambda = 1.06$ μm for two possible types of interaction. It can be seen that provided that a crystal of the needed orientation is available, it is possible to cover the whole mid-IR region with the spectrum of converted radiation.

Besides, the nonlinear susceptibility of centimeter-long crystals doubles as compared with the initial value of 23 pm/V and approaches 70 pm/V for 1-mm samples. This means that the layered structure decreases the GaSe nonlinear quality coefficient, in particular, at CO_2 laser SHG, by 5.4–8.9 times depending on the pump radiation wavelength.

In our opinion, new mixed nonlinear crystals $Hg_{(1-x)}Cd_xGa_2S_4$ (solid-state solution of $HgGa_2S_4$: : $CdGa_2S_4$) and $Ag_xGa_xGe_{(1-x)}S_2$ ($AgGaS_2$:GeS_2) are of particular interest for solution of the problem formulated.[13] Their important advantage is that varying the mixture ratio x, it is possible to obtain optimal noncritical phase-matching conditions for different types of PFC.

The transmission spectrum of a $6.5 \times 8 \times 2.1$ mm mixed $Hg_{0.65}Cd_{0.35}Ga_2S_4$ crystal of the point symmetry group $42m$ (see Fig. 2*a*) shifts toward shorter waves with respect to the initial $HgGa_2S_4$ crystal. Namely, the shortwave boundary at the zero level shifts to 460 nm, and the longwave one lies beyond the considered region, near 15 μm (see Fig. 2*b*). At the 10% level, the boundaries of the transmission spectrum were 495 nm and 13.2 μm.

The shortwave boundary does not change at transition from one measurement range on the entrance crystal surface to another. This crystal is more homogeneous with respect to this parameter than $HgGa_2S_4$. Transmittance variations are within 0.9%. At the same time, microelectronic-emission analysis showed significant (up to 20%) point-to-point variations of the Cd content. The optical loss coefficient can hardly be estimated for a crystal of such thickness, but it is at least no higher than 0.2 cm^{-1} in the maximum transmittance window at CO_2 laser wavelengths. In the absorption spectrum, a rather intense peak is observed at the wavelength of 2.1 μm, and this limits the capabilities of OPO pumped by a holmium laser. The coefficient of nonlinear susceptibility was determined to be 34 pm/V.

The studied biaxial $AgGaGeS_4$ crystal, as a representative of the second type of solutions at $x = 0.5$, has a point symmetry group $mm2$. The shortwave boundary of the transmission spectrum of a $10 \times 15 \times 2.1$ mm sample at the zero level lies nearby 440 nm (see Fig. 2*a*), and the longwave one is nearby 14 μm (see Fig. 2*b*). The boundaries at the 10% level are at 0.445 and 11.9 μm. The upper boundary of the absorption coefficient can be estimated as 0.2–0.3 cm^{-1}. In this case no absorption peak was found nearby 2 μm, as well as no polarization dependence of the transmission spectrum. At the wavelengths of the 9-μm CO_2 laser band, the optical loss is somewhat lower than in $ZnGeP_2$ and $LiInS_2$. A weak phonon absorption peak can be seen nearby 10.5 μm. At such a loss level the crystal is rather homogeneous. This is indicated by the presence of a clear shortwave boundary and immeasurably small variations of the transmission spectrum in the region of maximum transmittance. The results of the microelectronic-emission analysis showed that the crystal composition $Ag_{(1\pm0.019)}Ga_{(1\pm0.021)}Ge_{(1\pm0.012)}S_{(4\pm0.004)}$ in this case corresponds to the stoichiometric one accurate to ±2%.

Based on the Sellmeier dispersion formulas (see Table 2) it was found that the phase-matching conditions are fulfilled for the *e–oo* interaction in the planes *XZ* ($d_{\text{eff}} = d_{32}\sin\theta$) and *YZ* ($d_{\text{eff}} = d_{31}\sin\theta$), as well as for the *o–ee* interaction in the plane *XY* with $d_{\text{eff}} = d_{31}\sin^2\varphi + d_{32}\cos^2\varphi$. The nonlinear susceptibility coefficients d_{32} and d_{31} are equal to 8 and 12 pm/V, respectively. They are higher than in $LiInS_2$ [$d_{31} = 5.4$, $d_{33} = 6.2$, $d_{33} = 9.8$ pm/V (Ref. 14)].

4. Optical damage threshold

The lower nonlinear susceptibility of new crystals as compared with the known ones indicates that one of the decisive factors in the competition on the conversion efficiency is their optical damage threshold. In this connection, the optical damage threshold was measured carefully for 12 nonlinear crystals. A highly stabilized TEA CO_2 laser was used as a pump laser. At laser operation, the energy contribution of the pulse trailing edge did not exceed 10% and variations of the pulse energy during one measurement series were within 3.5%, those of the leading edge amplitudes were within 2%, and variations of the pulse duration (FWHM) did not exceed 2 ns (Ref. 15). The detailed description of our experimental technique on measurement of the optical damage threshold of the entrance surface of crystals can be found in Ref. 16. According to more accurate data, it turned out that the optical damage threshold of the known mid-IR crystals lies in a narrow ±15% range and equals 169 MW/cm^2 for Ag_3AsS_3, 157 for $CdGeAs_2$, 146 for $AgGaS_2$, 142 for $ZnGeP_2$, 139 for $AgGaSe_2$, 130 for CdSe, 121 for GaSe, and 68 MW/cm^2 for GaSe:In. For $AgGaGeS_4$ and $HgGa_2S_4$ (orange and yellow phases) and $Hg_{0.65}Cd_{0.35}Ga_2S_4$ it was 1.6, 2.2, 2.1, and 1.9 times higher than for $ZnGeP_2$, namely, 230, 310, 294, and 271 MW/cm^2.

Table 3 presents the estimated optical damage threshold normalized to $ZnGeP_2$ and multiplied by the figure of merit normalized to the same crystal for CO_2 laser SHG in some nonlinear crystals. Some parameters (for the first three crystals) given in the second, third, and fourth columns have been borrowed from Ref. 3.

Table 3. Comparative characteristics of nonlinear crystals for CO_2 laser SHG

Crystal	Transmission range $\Delta\lambda$, μm	Refractive index n (9–11 μm)	Birefringence, Δn	Square nonlinear coefficient d, pm/V	Effective nonlinear coefficient, d_{eff}, pm/V	Damage threshold I_d, rel. units	Figure of merit $M = d^2/n^3$, rel. units	$I_d \times M$, rel. units
$ZnGeP_2$	0.7–12 (2–11.2)	3.1	0.04	$d_{36} = 75$	≤30.5	1	1	1
$CdGeAs_2$	2.4–18 (4.5–16.5)	3.5	0.09	$d_{36} = 236$	104	1.15	8	9.5
$AgGaS_2$	0.47–13 (0.53–12.6)	2.34	0.05	$d_{36} = 12$	10	1.05	0.3	0.32
$AgGaGeS_4$	0.45–14.5 (0.5–13.5)	2.3	0.06	$d_{32} = 13$ $d_{31} = 8$	9.8	1.6	0.8	1.4
$LiInS_2$	0.45–15 0.55–13.5	2.2	0.06	$d_{33} = 12$ $d_{31} = 10$ $d_{32} = 6.5$	10.5	1.3	0.3	0.4
$HgGa_2S_4$	0.49–15.5 (0.55–13.5)	2.45	0.045	$d_{36} = 32$ $d_{31} = 12$	33	2.2	2.5	5.5

The second column gives two transmission regions for each crystal: the first corresponds to the fundamental transmittance boundaries caused by the electron and phonon absorption, and the second (in parentheses) is the real possible region for the processes of parametric frequency conversion that is caused by up-to-date technological capabilities of crystal growth. The equations for the effective nonlinear coefficient d_{eff} for the first type of three-frequency nonlinear interactions have the form:

$$d_{36} \sin 2\theta \cos 2\varphi \ (ZnGeP_2 \text{ and } CdGeAs_2),$$

$$d_{36} \sin 2\theta \sin 2\varphi \ (AgGaS_2),$$

$$d_{32} \cos^2\varphi + d_{31} \sin^2\varphi \ (AgGaGeS_4 \text{ in the plane } XY),$$

$$d_{32} \cos^2\varphi + d_{31} \sin^2\varphi \ (LiInS_2 \text{ in the plane } XZ),$$

$$d_{36} \sin\theta \sin 2\varphi + d_{31} \sin 2\theta \cos 2\varphi \ (HgGa_2S_4).$$

It is well-known that in the set of operation features (the need in cryogenic cooling), in the technology of monocrystal growth (the optical loss coefficient up to 0.5 cm^{-1} at the second harmonic wavelengths), and other parameters, the $CdGeAs_2$ crystals yield to the $ZnGeP_2$ crystals.[3] In this connection, let us compare the potential efficiency of the crystals studied with respect to the leader.

The crystal figure of merit multiplied by the optical damage threshold, as well as both these parameters separately, is proportional to the efficiency of frequency conversion and demonstrates more than fivefold superiority of $HgGa_2S_4$ over $ZnGeP_2$. The same superiority should be expected from the mixed $Hg_{0.65}Cd_{0.35}Ga_2S_4$ crystal because of its close nonlinear susceptibility (the initial crystals have the same susceptibility). Thanks to the low values of the refractive indices, closeness of the phase-matching angles to the noncritical 90° angle, in spite of significantly lower nonlinear properties, the potential efficiency of SHG in $AgGaGeS_4$ turns out to be 1.4 times higher than in $ZnGeP_2$.

Unlike the crystals described above, all the three new crystals, as well as GaSe, are suitable for initiation of mid-IR OPOs when pumping by solid-state lasers, in particular, by a Nd:YAG laser, for the first time. Potentially, the $HgGa_2S_4$ crystals are most efficient. The low optical damage threshold of the GaSe:In crystals with respect to GaSe is caused only by imperfection of the doping technology. Its further development and, at least, reservation of the optical damage threshold of the initial GaSe crystals will cause the superiority of this crystal with respect to $ZnGeP_2$ at CO_2 laser SHG. The possibility of the OPO initiation is caused by the region of spectral transmission of the crystals.

Conclusions

Thus, based on the results of investigation of physical properties of poorly studied nonlinear $HgGa_2S_4$ crystals, new mixed nonlinear $AgGaGeS_4$ crystals from the $AgGa_{1-x}Ge_xS_4$ family at $x = 0.5$ and $Hg_{0.65}Cd_{0.35}Ga_2S_4$ crystals from the $Hg_{(1-x)}Cd_xGa_2S_4$ family, their applicability is demonstrated for the first time to initiate high-efficiency mid-IR OPOs when pumping by solid-state lasers, in particular, by a Nd:YAG laser.

Because of opaqueness or high optical loss of the known crystals, the potential advantage is demonstrated for second harmonic generation of CO_2 laser, as an example. For the $HgGa_2S_4$ crystals, it is fivefold as compared with $ZnGeP_2$. It is obvious that perfection of the technology of growing high-quality doped GaSe:In crystals will allow the same conclusion to be drawn as well.

The use of Nd:YAG laser frequency converters based on new crystals into the mid-IR spectral region in combination with the existing frequency converters into the UV region that are based on LBO, KTA, KTP, and

BBO crystals opens the possibility for creation of coherent radiation sources in the region of 0.2–12.0 μm. Such radiation sources can be used for the development of versatile gas-aerosol lidars.

References

1. V.E. Zuev, M.V. Kabanov, Yu.M. Andreev, V.G. Voevodin, P.P. Geiko, A.I. Gribenyukov, and V.V. Zuev, Izv. Akad. Nauk SSSR, Ser. Fiz. **52**, No. 6, 1142–1149 (1988).
2. Yu.G. D'yakova, M.A. Ambartsumyan, E.K. Belonogova, and T.N. Miroshnichenko, Laser News, No. 6, 3–32 (2000).
3. V.G. Dmitriev, G.G. Guzadyan, and D.N. Nikogosyan, *Handbook of Nonlinear Optical Crystals* (Springer Verlag, New York–Berlin–Heidelberg, 1999).
4. Yu.M. Andreev, L.M. Butkevich, V.G. Voevodin, A.V. Voitsekhovskii, V.P. Voronkov, A.P. Vyatkin, A.A. Eliseev, V.E. Zuev, V.V. Zuev, M.V. Kabanov, T.N. Kopylova, G.V. Maier, A.N. Morozov, A.S. Petrov, O.V. Ravodina, A.P. Serykh, I.V. Sokolova, and N.P. Soldatkin, *Componentry of Optoelectronic Devices* (RASKO, Tomsk, 1992), 294 pp.
5. M.C. Ohmer and R. Pandey, MRS Bulletin, No. 7, 16–22 (1998).
6. K.L. Vodopyanov and V.G. Voevodin, Opt. Commun. **114**, February 1, 333–335 (1995).
7. V.V. Badikov, I.N. Matveev, V.L. Panyutin, S.M. Pshenichnikov, T.M. Repyakhova, O.V. Rychik, A.E. Rozenson, N.K. Trotsenko, and N.D. Ustinov, Kvant. Elektron. **6**, No. 8, 1807–1809 (1979).
8. D.R. Suhre, N.B. Singh, V. Balakrisha, N.C. Fernelius, and F.K. Hopkins, Opt. Lett. **22**, No. 11, 775–777 (1997).
9. V.V. Badikov, A.G. Tyulyupa, G.S. Shevyrdyaeva, and S.G. Sheina, Izv. Akad. Nauk SSSR, Ser. Neorgan. Material. **27**, No. 2, 248–252 (1991).
10. Yu.M. Andreev, L.G. Geiko, P.P. Geiko, and S.G. Grechin, Kvant. Elektron. **31**, No. 7, 647–648 (2001).
11. K.L. Vodopyanov and V. Chazapis, Opt. Commun. **135**, 98–102 (1997).
12. Yu.M. Andreev, S.A. Bereznaya, V.G. Voevodin, P.P. Geiko, and M.V. Kabanov, in: *Proc. of the Second Int. Symp. on Monitoring and Rehabilitation of the Environment* (IOM SB RAS, Tomsk, 2000), pp. 56–57.
13. Yu.M. Andreev, V.V. Badikov, P.P. Geiko, L.G. Geiko, V.V. Panyutin, and G.S. Shevyrdyaeva, in: *Proc. of the Fifth Korea-Russia Int. Symp. on Science and Technology* (TPU, Tomsk, 2001), pp. 290–294.
14. L. Isaenko, I. Vasilieva, A. Yelisseyev, S. Labanov, V. Malakhov, L. Dovlitova, J.J. Zondy, and I. Kavun, J. Cryst. Growth **218**, 313–322 (2000).
15. A.I. Karapuzikov, A.V. Malov, and I.V. Sherstov, Infrared Phys. Technol. **41**, No. 2, 77–85 (2000).
16. Yu.M. Andreev, V.V. Badikov, V.G. Voevodin, L.G. Geiko, P.P. Geiko, M.V. Ivashchenko, A.I. Karapuzikov, and I.V. Sherstov, Kvant. Elektron. **31**, No. 12, 1075–1078 (2001).